coatings

MDPI

Article

Surface Modification of Titanium by Micro-Arc Oxidation in Promoting Schwann Cell Proliferation and Secretion of Neurotrophic Factors

Cong Dong [1,†], Shenghao Xue [1,†], Binbin Kang [2], Xinyuan Zhang [1], Qun Zhong [1], Xiaohong Chen [2,*] and Shengcai Qi [1,*]

[1] Shanghai Key Laboratory of Craniomaxillofacial Development and Diseases, Department of Prothodontics, Shanghai Stomatological Hospital & School of Stomatology, Fudan University, Shanghai 200437, China
[2] School of Materials and Chemistry, University of Shanghai for Science & Technology, Shanghai 200093, China
* Correspondence: cxh992@usst.edu.cn (X.C.); qishengcai@fudan.edu.cn (S.Q.)
† These authors contributed equally to this study.

Abstract: Titanium and its alloys have been widely used in the field of oral implants over the past few decades. However, the effect of micro-arc oxidation modified titanium surface on Schwann cells has not been studied, which is of great significance for nerve regeneration around implants and improvement of osseoperception. In this study, the characterization of the titanium surface modified by micro-arc oxidation (MAO) was detected by scanning electron microscope (SEM), XPS and a contact angle measurement system. Schwann cells (SCs) were cultured on titanium surfaces of micro-arc oxidation (MAO) and pure titanium (Ti). At different time points, the morphology and adhesion of SCs on the titanium surfaces were observed by SEM. Cell proliferation activity was detected by the CCK-8 method. The expression levels of mRNA and proteins of nerve growth factor (NGF) and glial-derived neurotrophic factor (GDNF) were detected by RT-PCR, immunofluorescence and western blot. The results of this in vitro study revealed that micro-arc-oxidation-modified titanium surfaces promoted Schwann cell proliferation and secretion of neurotrophic factors compared with pure titanium. CCK-8 results showed that the number of Schwann cells on MAO surfaces was significantly higher than that of the Ti group on day 7. The mRNA expressions of *Ngf* and *Gdnf* were up-regulated in both groups from day 1 to day 7. On day 3 and day 7, the gene expression of *Ngf* in the MAO group was significantly higher than that of the Ti group. On day 7, the MAO group appeared significantly up-regulated in gene expression level of *Gdnf*. The results of western blot were consistent. Micro-arc oxidation modification provides an accurate and effective method for promoting nerve regeneration of titanium microtopography coatings, which have potential significance for promoting patients' osseoperception ability in clinical practice.

Keywords: micro-arc oxidation; Schwann cell; proliferation; NGF; GDNF

Citation: Dong, C.; Xue, S.; Kang, B.; Zhang, X.; Zhong, Q.; Chen, X.; Qi, S. Surface Modification of Titanium by Micro-Arc Oxidation in Promoting Schwann Cell Proliferation and Secretion of Neurotrophic Factors. *Coatings* **2022**, *12*, 1797. https://doi.org/10.3390/coatings12121797

Academic Editor: Jun-Beom Park

Received: 10 October 2022
Accepted: 15 November 2022
Published: 22 November 2022

1. Introduction

With the development of implant technology, people are increasingly pursuing biofunctional oral implants. Patients with oral implants are not only satisfied with the masticatory function restored by osseointegration, but also desirous to obtain a tactile sensory ability closer to the natural teeth. Although the osseointegration can be effectively enhanced by different titanium surface modification, suitable loading protocols, and peri-implant cytokine interfering [1–4], there still exist clinical cases in which implants with intact osseointegration have failed due to excessive bite force [5]. At the same time, the tactile sensory ability of implants is only 1/50–1/10 of natural teeth [6]. This special type of sensory ability of implants is named "osseoperception", and is considered closely related to the nerve regeneration around the implant [7].

Although tooth extraction leads to the damage of myelinated nerve fibers, nevertheless, the remaining nerve fibers and their endings in the alveolar bone and periodontal ligament residue might be able to regenerate and partially recover the sensory feedback [7]. Previous studies suggested that the stimulation of functional implants resulted in an accelerated proliferation of adjacent Schwann cells, and the loading pressure regenerated nerve fibers surrounding the implants, allowed axon differentiation and guided sprouting to connect with Schwann cells [8]. A recent study showed the number of mature and newly regenerated nerve fibers around the implant gradually increased with the process of osseointegration, and the innervation in the soft tissue took place faster than in the bone tissue [9]. Research also found that an immediate implantation and loading protocol was most beneficial to the innervation of the peripheral nerve around the implant, and the myelinated nerve density in the apical region was the highest. It was also found that peri-implant nerve regeneration and osseointegration were inhibited in rats receiving inferior alveolar neurectomy [10,11]. To sum up, nerve regeneration around the implant is closely related to osseoperception. However, so far no effective implant surface treatment has been reported could promote nerve regeneration around the implant.

Micro-arc oxidation (MAO), a cost-effective electrochemical treatment, has been widely applied to valve metals such as titanium, zirconium, tantalum and niobium. In the process of treatment, the metal surface maintains the anode condition, which is higher than the dielectric breakdown barrier, and promotes the plasma spark at the interface metal electrolyte. The plasma sparking and oxidation reaction can generate a thick porous oxide film, which is strongly bonded to the substrate [12,13]. The content of each element doped in the coating can be controlled by adjusting the electrolyte composition. Micro/nanoscale porous structures and elements doped onto a titanium surface by MAO can endow the coating with a bidirectional regulatory function, and improve the compatibility and antibacterial properties of implants [14]. Our team's previous research revealed that Zn-TiO_2 coatings possess excellent antibacterial properties against *Staphylococcus aureus* (*S. aureus*) and *Porphyromonas gingivalis* (*P. gingivalis*) [15].

Schwann cells play an irreplaceable role in nerve regeneration and nerve injury repair [16]. During development, Schwann cells are associated with a bundle of axons and release a variety of neurotrophic factors, such as nerve growth factor (NGF) and glial-cell-line-derived neurotrophic factor (GDNF), which are involved in axonal growth and pathfinding [17]. Researchers found the function of Schwann cells could be enhanced by various titanium implant surfaces [18]. A study revealed that TiO_2 nanotubes loaded with a concentration of 20 μg/mL minocycline increased Schwann cell proliferation and secretion of neurotrophic factors in vitro [19]. However, the effect of a MAO-modified titanium surface on Schwann cells has been rarely studied. The purpose of this study was to explore whether there is a direct interaction between the MAO-modified titanium surface and Schwann cells to provide a means for subsequent implant surface modification and to promote nerve regeneration and maturation.

In this study, Ti-incorporated coatings (Ti-MAO) on the oral implant surface were prepared by a micro-arc oxidation technique, and the proliferation of Schwann cells on the MAO-modified titanium, as well as their ability to secrete neurotrophic factor, was analyzed in vitro.

2. Materials and Methods

2.1. MAO-Modified Titanium Surface Preparation

Titanium plates with diameters of 14 mm were cut from commercial pure titanium sheets (cp Ti, TA4) and ground gradually with 1200 # SiC sandpaper. Then, before treatment, the samples were ultrasonically cleaned with acetone, absolute ethanol and distilled water. An aqueous electrolyte consisting of 20 g/L trisodium phosphate dodecahydrate ($Na_3PO_4 \bullet 12H_2O$) and 4 g/L sodium hydroxide (NaOH) was prepared as the electrolyte. MAO was executed by DC power supply. A stainless steel plate was used as the cathode plate and a titanium sample was used as the anode. The electrolyte temperature was

maintained at 30 °C through the circulating water treatment system. Manufacture took place for 5 min at a constant voltage of 400 V. After that, the samples were ultrasonically cleaned with deionized water for 5 min, dried, and stored at room temperature until use. More details can be found in our previous research [15].

2.2. Surface Characterization

2.2.1. Surface Morphology Measurements

All the samples were thoroughly rinsed with deionized water and then dried at room temperature. The surface morphology of the samples was characterized by scanning electron microscopy (Hitachi S-4800, Hitachi, Tokyo, Japan).

2.2.2. Chemical Composition and X-ray Diffraction Measurements

Chemical compositional analysis was undertaken by XPS (ESCALAB 250XI, Thermo Scientific, Waltham, MA, USA). The phase composition analysis of all coatings was performed by X-ray diffraction (XRD, D8 ADVANCE, Bruker, Munich, Germany).

2.2.3. Wettability Measurements

The surface wettability was measured by contact angles. Contact angle measurements were conducted and analyzed by a contact angle measurement system (SEO Phoenix 300, SEO, Seoul, Korea). One droplet (4 μL) of deionized water was added on top of the substrates. The contact angle was immediately measured 5 s after placing the drop on each sample and the test was conducted at room temperature. Measurements were performed three times; the average contact angle was determined.

2.3. Cell Assays

2.3.1. Cell Culture

Schwann cells (SCs) were used for all cell experiments. Cells were cultured at 37 °C in a humidified, 5% CO_2/95% air environment (CI191C, Thermos Fisher Scientific, Waltham, MA, USA).

2.3.2. Cell Viability Assays

In order to analyze the cell viability, all sterilized Ti and MAO plates (14 mm in diameter) were put into the holes of 24-well tissue culture plates. The samples were washed twice with PBS. Then, with a density of 2.5×10^4 cells/plate, cells were inoculated onto the samples. During the proliferation trials, the medium was changed every other day. After 1, 3 and 7 days of incubation, CCK-8 dye was added to each well, and then incubated at 37 °C for 4 h, and optical density (OD) was measured at 450 nm with a panel reader.

2.3.3. Scanning Electron Microscope/Confocal Laser Scanning Microscope Assays

The cells were diluted to 2.5×10^4 cells/plate for seeding on the material surface. After culturing for 1, 3, and 7 days, the medium was discarded and washed 3 times with PBS. The titanium plates were transferred to a new 24-well plate with sterile forceps, then 2.5% glutaraldehyde was added and kept at 4 °C overnight. Then the plates were rinsed with PBS three times, and in turn, 50%, 60%, 70%, 80%, 90%, 100% ethanol was added, acting for 10 min, with 100% ethanol used × 2 times. Then the samples were taken out and put into a freeze dryer for 6 or 7 h to complete the sample preparation for the SEM assays.

In the same way, after culturing for 1, 3 and 7 days, the medium was discarded and the samples were washed with PBS twice. The cells were fixed in 4% paraformaldehyde for 30 min and then cultured with Triton X-100 for 10 min. After this, all cells were treated with 5% goat serum to block nonspecific antibodies. The plates were incubated with antibodies NGF (1:500, Abcam, UK) and GDNF (1:250, Abcam, UK) overnight. The samples were then incubated with the corresponding fluorescein-conjugated secondary antibody and phalloidin at room temperature in the dark, which were subsequently analyzed with a confocal laser scanning microscope (Leica TCS SP8, Leica, Heidelberg, Germany).

2.4. Molecule Assays

2.4.1. Real-Time PCR

Each group of specimens was put into a 6-well plate, and then the Schwann cells were inoculated on the surface of different plates at a density of 1×10^5 per well at 37 °C in a humidified atmosphere of 5% CO_2. After 1, 3 and 7 days of culture, total RNA was extracted from the treated cells using TRIzol reagent for 10 min (Invitrogen, Carlsbad, CA, USA). Then, 200 µL chloroform was added, and the samples were centrifuged at 4 °C at 12,000 rpm for 15 min. The colorless upper aqueous phase was transferred to a fresh test tube and was mixed with 500 µL isopropyl alcohol. The samples were centrifuged at 4 °C under 12,000 rpm for 15 min, and then the supernatant was removed. Following this, 500 µL 75% ethanol was used to wash RNA pellets and then dissolved in 10 µL diethylpyrocarbonate-treated water. The Revert Aid kit (Takara Bio, Otsu, Japan) was used according to the manufacturer's instructions to reverse-transcribe RNA into cDNA. qPCR was performed on an ABI Prism 7500 detection system with Universal SYBR® Green. The mRNA level of cells cultured on pure titanium plates on the first day was taken as the baseline. Fold changes at mRNA level were calculated using a $2^{-\Delta\Delta Ct}$ method. The primer sequences are shown in Table 1.

Table 1. The primers for genes used in quantitative real-time RT-PCR.

Primer	Sequence(5′-3′)
GAPDH-F	GGCACAGTCAAGGCTGAGAATG
GAPDH-R	ATGGTGGTGAAGACGCCAGTA
NGF-F	TCAACAGGACTCACAGGAGCA
NGF-R	GGTCTTATCTCCAACCCACACAC
GDNF-F	CAGAGGGAAAGGTCGCAGAG
GDNF-R	ATCAGTTCCTCCTTGGTTTCGTAG

2.4.2. Western Blot

The protein expression of GDNF and NGF was detected by western blot analysis. Each group of specimens was placed in 6-well plates, and then Schwann cells were inoculated on the titanium plates at 1×10^5 cells per well. After 1, 3 and 7 days of culture, the total protein was separated using RIPA lysis buffer (Biosharp, Shanghai, China) supplemented with protease inhibitor and phosphatase inhibitor (Beyotime, Shanghai). The protein concentration was determined using the DIINDANEDIAC ACID PROTEIN DETECTION KIT (Beyoutham, Shanghai, China). An equivalent amount of protein (50 µg) was separated by SDS-PAGE electrophoresis, and then transferred to PVDF film (Millipore, Bedford, MA, USA). The membrane was sealed with 5% non-fat emulsion in TBST (0.1% Triton X-100 in TBS) buffer solution for 90 min, and then incubated at 4 °C with primary antibodies against NGF (rabbit anti rat, 1:400, abcam, UK) and GDNF (rabbit anti rat, 1:400 abcam, UK) overnight. Then, the membrane was cultured with horseradish peroxidase and a secondary antibody (goat anti rabbit, 1:5000, abcam, UK), and visualized with ECL reagent (Proteintech, US). The band strength representing the protein level was evaluated using GelPro Analyzer 3.0 (Media Controls, Rockville, MD, USA). GAPDH was used to normalize target proteins.

2.5. Statistical Analysis

All analyses were made in triplicate and repeated at least three times. Data were collected and significant differences were evaluated using ANOVA, and one-tailed Student's *t*-tests were performed. The statistical significance was considered at $p < 0.05$.

3. Results

3.1. Surface Characterization

Figure 1A shows the surface morphologies of MAO coating under SEM, which indicate that the MAO coating has a microporous structure. The results of XRD showed that MAO coating mainly consisted of anatase and rutile (Figure 1B). According to the full spectrum XPS results, we found that Ti, O, P and C were detected on the surfaces (Figure 1C). The wettability of the MAO coating is determined by the water contact angle shown in Figure 1D. The contact angle of the MAO coating is about 43°.

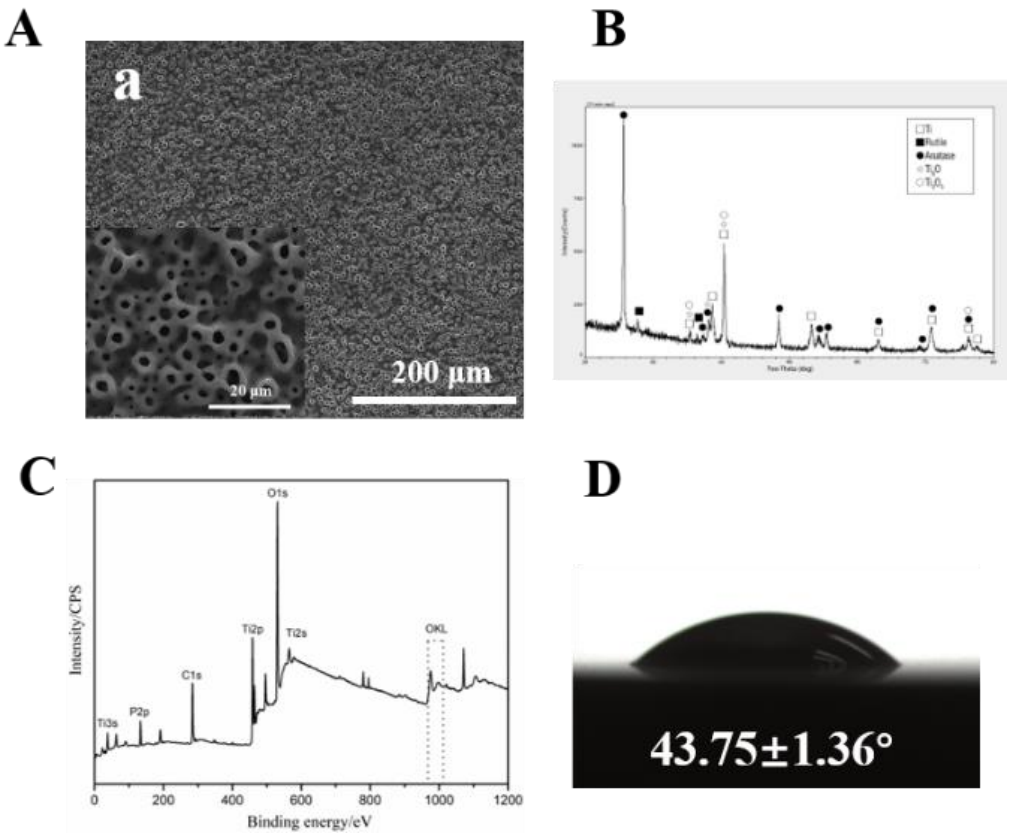

Figure 1. Surface morphologies (**A**), XRD patterns (**B**), XPS survey spectrum (**C**), and digital photograph of water droplets of MAO coating (**D**).

3.2. Cell Assays

3.2.1. Cell Viability and Scanning Electron Microscope Assays

Figure 2A,B show that the antennae of Schwann cells extend into the micropores on the surface of MAO, whereas on the surface of pure titanium, Schwann cells seem to be unable to extend, scattered and distributed in different shapes. The results of CCK-8 show that the number of cells in the two groups gradually increased on days 1, 3, and 7 of culture. There was no significant difference in the number of cells between the two groups on days 1 and 3, whereas on day 7, the number of cells in the MAO group was significantly higher than that in the Ti group.

As shown in the Figure 3, the quantity of the two groups' cells gradually increased on days 1, 3 and 7 of culture. Schwann cells on the Ti surfaces remained spherical throughout and appeared to be less stretched. On the MAO surface, the cells stretched obviously; on day 7, they formed clumps and were closely connected with each other. On the Ti surface, although the number of cells increased, they were spherical and less connected compared with those on the MAO surface.

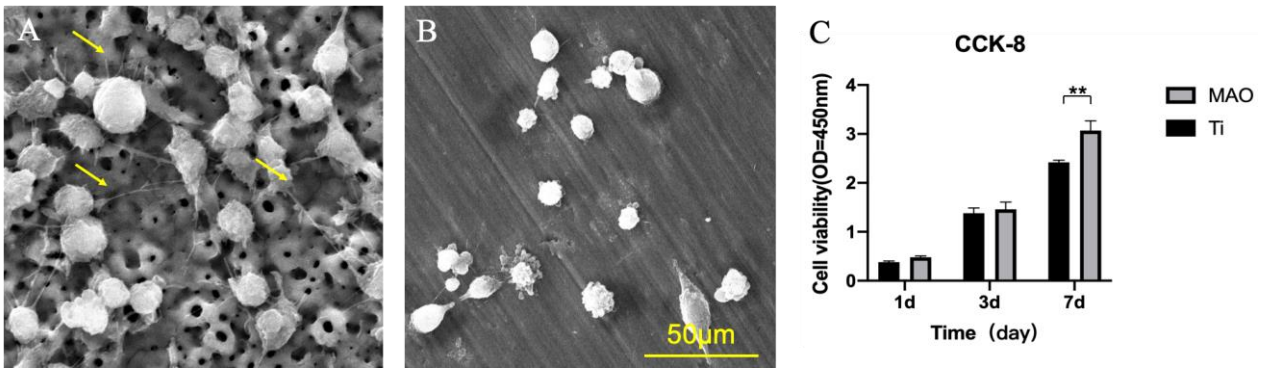

Figure 2. The growth pattern and morphology of Schwann cells on MAO (**A**) and Ti (**B**) surfaces, and the result of CCK-8 (**C**). ("**" means $p < 0.01$).

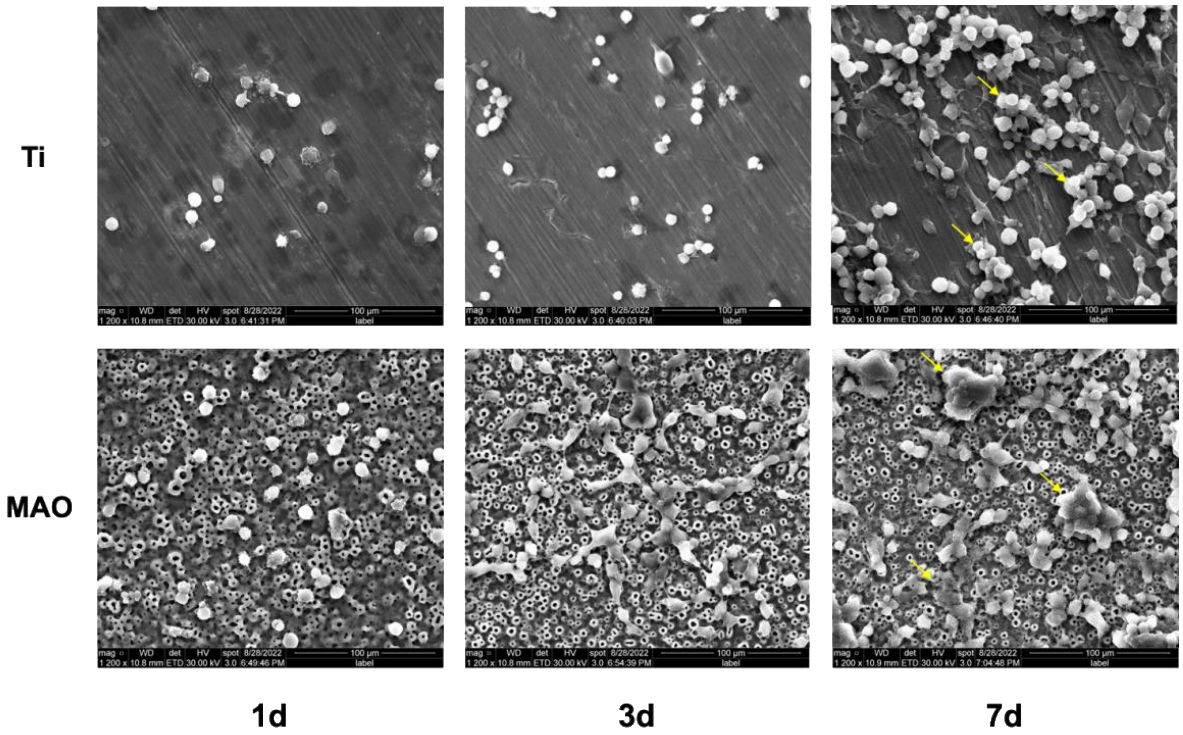

Figure 3. The quantity and morphology of Schwann cells on MAO and Ti surfaces on days 1, 3 and 7 of culture by SEM.

3.2.2. Confocal Laser Scanning Microscope Assays

It can be seen from the Figure 4 that the proliferation and differentiation of Schwann cells gradually increased with time. On different days of culture, the strength of the phalloidin-labeled actin filaments in the MAO group was higher than that in the Ti group, indicating the former had better extension ability for SCs. In the MAO group, Schwann cells' antennas grew clearly on the third day of culture, the degree of cytoskeleton extension was much higher than that of the Ti group, and expression of NGF and GDNF was also increased. At the same time, NGF and GDNF could be seen evenly distributed in the nucleus and cytoplasm of SCs.

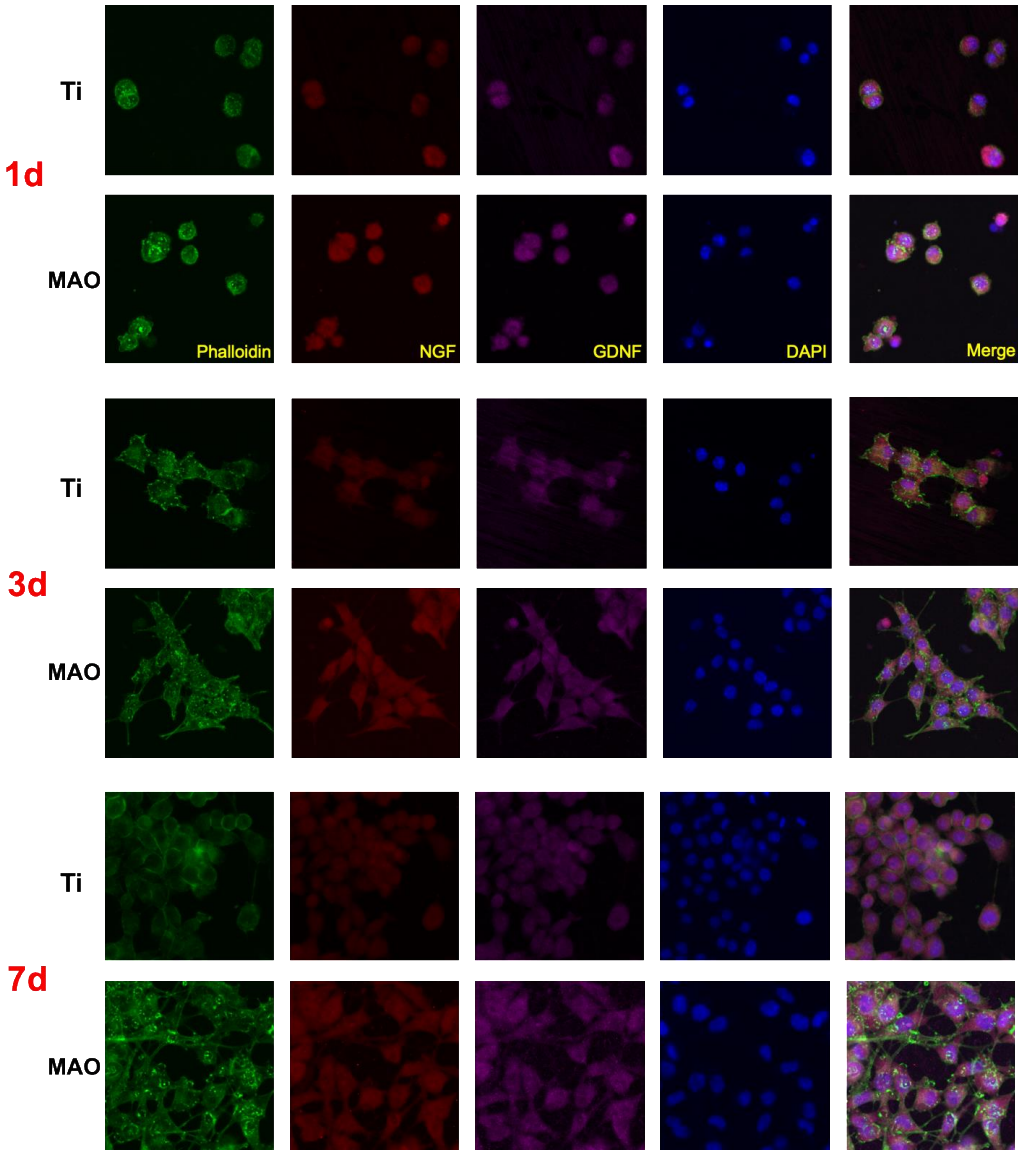

Figure 4. The morphology and expression of NGF and GDNF of Schwann cells on MAO and Ti surfaces on days 1, 3 and 7 of culture by CLSM.

3.3. Molecules Assays

3.3.1. Real-Time PCR

As seen from Figure 5, the mRNA expression of *Ngf* and *Gdnf* was up-regulated in both groups from day 1 to day 7. On the seventh day, the gene expression of *Ngf* and *Gdnf* in the MAO group was significantly higher than that in the Ti group, which were 12-fold and 5.5-fold of the first day, respectively. Furthermore, it was also much higher than the gene expression level on days 1 and 3, especially the *Ngf* of the third day in the MAO group.

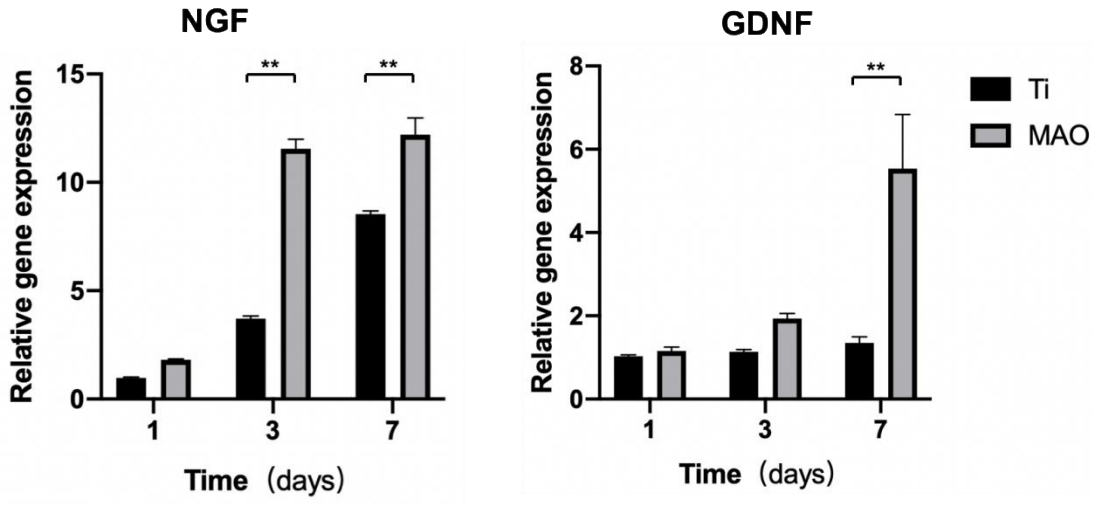

Figure 5. Gene expression level of *Ngf* and *Gdnf* in Schwann cells on days 1, 3 and 7 by real-time PCR (mean ± SD, $n = 6$). The mRNA expression of *Ngf* and *Gdnf* was up-regulated in both groups from day 1 to day 7. On the third and seventh days, the gene expression of *Ngf* in the MAO group was significantly higher than that in the Ti group. On the seventh day, the MAO group appeared significantly up-regulated in the gene expression level of *Gdnf*. ("**" means $p < 0.01$).

3.3.2. Western Blot

Figure 6 shows the effect of the MAO surface on the protein expression of NGF and GDNF on days 1, 3 and 7. The protein expression of NGF had no significant difference on day 1, but was up-regulated obviously on days 3 and 7. Meanwhile, the expression of GDNF increased on the third day compared with the control group, but there was no obvious difference on the first and seventh days.

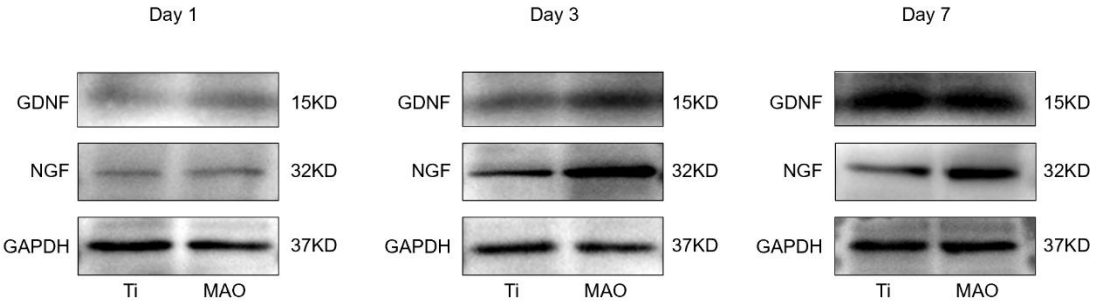

Figure 6. Protein expression level of NGF and GDNF in Schwann cells on days 1, 3 and 7 by western blot (mean ± SD, $n = 6$). GAPDH was used to normalize target proteins. Compared with the control group, the protein expression of NGF and GDNF was up-regulated, especially NGF, in the MAO group on day 3 and day 7.

4. Discussion

With the development of implant restoration technology, it is hoped that implants can gain sensory function [20]. Studies have shown that there is a certain neural perception ability around implants, but this perception ability is weaker than that of natural teeth, which will lead to long-term overloading of dental implants during use, resulting in mechanical complications such as superstructure collapse and implant fracture, and even the destruction of the alveolar bone around the implant, causing irreversible damage [21,22]. Therefore, there is an urgent need to improve the osseoperception of implants and avoid the risks caused by weak sensory ability.

Owing to the ability of regulating neuronal development in peripheral nerves, Schwann cells were selected for study [20]. When nerve fibers are cut, the distal Schwann cells form Büngner bands that guide axons to regenerate and extend to target organs. Therefore,

promoting the peri-implant growth of Schwann cells is a tool for achieving peri-implant nerve regeneration [23].

In our study, MAO coatings prepared on pure titanium were distributed with micro-scale pores, which can significantly promote Schwann cells' adhesion and morphology differentiation (Figure 2). In addition, the volcano-shaped micropores can provide the desired spatial environment for the proliferation and adhesion of different cells [24,25]. The contact angle of the MAO coatings was 43° (Figure 1d), which is hydrophilic. Hydrophilic surfaces are beneficial in the early stages of osseointegration [26], which would be suitable for neural cells' adhesion to the implant surface. The cell viability of SCs on the MAO coating was much higher than that in the Ti group on days 1, 3 and 7 of culture (Figure 2c). The results of SEM assays showed that the antennae of Schwann cells extend into the micropores on the surface of MAO, whereas on the surface of pure titanium, Schwann cells seem to be unable to extend, which showed good cellular biocompatibility of the MAO coatings in our study.

In the CLSM assays, multiple immunofluorescence staining was used: phalloidin was selected to mark the cytoskeleton to show cell extension, and two other common neurotrophin factors, NGF and GDNF, were used to mark the expression of neural-related factors in Schwann cells. In the MAO group, Schwann cells' antennas grew clearly on the third day of culture, the degree of cytoskeleton extension was much higher than that of the Ti group, and expression of NGF and GDNF was also increased. At the same time, NGF and GDNF could be seen evenly distributed in the nucleus and cytoplasm of SCs. It has been confirmed that the GDNF and NGF released from SCs exerted a synergistic effect on promoting neural differentiation [19,27]. Meanwhile, Zhigang Wu found that Schwann cells can promote the migration, proliferation and differentiation of bone marrow stromal cells (BMSCs), which suggests that Schwann cells would not interfere with the process of osseointegration [28]. All of these results showed that MAO coatings significantly promote the expression of NGF and GDNF of SCs, which needs further research in future.

In conclusion, osseoperception in implants is the key to avoiding the risks caused by weak sensory ability. In our study, it was found that MAO coating improves the adhesion, proliferation and secretion of neurotrophic factor of SCs in vitro, which may improve the osseoperception of implants in a clinical setting.

Author Contributions: Conceptualization, S.X. and C.D.; methodology, S.X., C.D., X.Z. and B.K.; investigation, S.Q.; data curation, S.X.; writing—original draft preparation, S.X.; writing—review and editing, C.D.; supervision, X.C.; project administration, Q.Z.; funding acquisition, S.Q. All authors have read and agreed to the published version of the manuscript.

Funding: This research was funded by the Science and Technology Innovation Talent Training Program of Shanghai Stomatological Hospital (SSH-2022-KJCX-B05).

Institutional Review Board Statement: Not applicable.

Informed Consent Statement: Not applicable.

Data Availability Statement: All data that support the findings of this study are included within the article.

Conflicts of Interest: The authors declare no conflict of interest.

References

1. Ye, J.; Huang, B.; Gong, P. Nerve Growth Factor-Chondroitin Sulfate/Hydroxyapatite-Coating Composite Implant Induces Early Osseointegration and Nerve Regeneration of Peri-Implant Tissues in Beagle Dogs. *J. Orthop. Surg. Res.* **2021**, *16*, 51. [CrossRef] [PubMed]
2. Song, D.; Liang, X.; Zheng, H.; Shujaat, S.; Dessel, J.V.; Zhong, W.; Ma, G.; Lambrichts, I.; Jacobs, R. Peri-Implant Myelinated Nerve Fibers: Histological Findings in Dogs. *J. Periodontal Res.* **2020**, *55*, 567–573. [CrossRef] [PubMed]
3. Ma, T.; Ge, X.-Y.; Hao, K.-Y.; Zhang, B.-R.; Jiang, X.; Lin, Y.; Zhang, Y. Simple 3,4-Dihydroxy-L-Phenylalanine Surface Modification Enhances Titanium Implant Osseointegration in Ovariectomized Rats. *Sci. Rep.* **2017**, *7*, 17849. [CrossRef] [PubMed]

4. Zhang, Y.; Xu, J.; Ruan, Y.C.; Yu, M.K.; O'Laughlin, M.; Wise, H.; Chen, D.; Tian, L.; Shi, D.; Wang, J.; et al. Implant-Derived Magnesium Induces Local Neuronal Production of CGRP to Improve Bone-Fracture Healing in Rats. *Nat. Med.* **2016**, *22*, 1160–1169. [CrossRef]
5. Guglielmotti, M.B.; Olmedo, D.G.; Cabrini, R.L. Research on Implants and Osseointegration. *Periodontol 2000* **2019**, *79*, 178–189. [CrossRef] [PubMed]
6. Negahdari, R.; Ghavimi, M.; Ghanizadeh, M.; Bohlouli, S. Active Tactile Sensibility of Three-Unit Implant-Supported FPDs versus Natural Dentition. *J. Clin. Exp. Dent.* **2019**, *11*, e636–e641. [CrossRef] [PubMed]
7. Song, D.; Shujaat, S.; Politis, C.; Orhan, K.; Jacobs, R. Osseoperception Following Dental Implant Treatment: A Systematic Review. *J. Oral Rehabil.* **2021**, *49*, 573–585. [CrossRef] [PubMed]
8. Zaminy, A.; Shokrgozar, M.A.; Sadeghi, Y.; Noroozian, M.; Heidari, M.H.; Piryaei, A. Mesenchymal stem cells as an alternative for Schwann cells in rat spinal cord injury. *Iran. Biomed. J.* **2013**, *17*, 113–122.
9. Li, J.; Xue, S.; Liu, Z.; Yao, D.; Jiang, T. Distribution of Mature and Newly Regenerated Nerve Fibres after Tooth Extraction and Dental Implant Placement: An Immunohistological Study. *J. Oral Rehabil.* **2022**, *49*, 796–805. [CrossRef] [PubMed]
10. Huang, Y.; van Dessel, J.; Martens, W.; Lambrichts, I.; Zhong, W.-J.; Ma, G.-W.; Lin, D.; Liang, X.; Jacobs, R. Sensory Innervation around Immediately vs. Delayed Loaded Implants: A Pilot Study. *Int. J. Oral Sci.* **2015**, *7*, 49–55. [CrossRef] [PubMed]
11. Liu, Y.; Zheng, G.; Liu, L.; Wang, Z.; Wang, Y.; Chen, Q.; Luo, E. Inhibition of Osteogenesis Surrounding the Titanium Implant by CGRP Deficiency. *Connect. Tissue Res.* **2018**, *59*, 147–156. [CrossRef] [PubMed]
12. Shimabukuro, M. Antibacterial Property and Biocompatibility of Silver, Copper, and Zinc in Titanium Dioxide Layers Incorporated by One-Step Micro-Arc Oxidation: A Review. *Antibiotics* **2020**, *9*, 716. [CrossRef] [PubMed]
13. Hanawa, T. Titanium-Tissue Interface Reaction and Its Control with Surface Treatment. *Front. BioEng. Biotechnol.* **2019**, *7*, 170. [CrossRef] [PubMed]
14. Zhang, L.; Guo, J.; Yan, T.; Han, Y. Fibroblast responses and antibacterial activity of Cu and Zn co-doped TiO_2 for percutaneous implants. *Appl. Surf. Sci.* **2018**, *434*, 633–642. [CrossRef]
15. Kang, B.; Lan, D.; Liu, L.; Dang, R.; Yao, C.; Liu, P.; Ma, F.; Qi, S.; Chen, X. Antibacterial Activity and Bioactivity of Zn-Doped TiO_2 Coating for Implants. *Coatings* **2022**, *12*, 1264. [CrossRef]
16. Dubový, P.; Klusáková, I.; Hradilová-Svíženská, I.; Joukal, M. Expression of Regeneration-Associated Proteins in Primary Sensory Neurons and Regenerating Axons After Nerve Injury—An Overview. *Anat. Rec.* **2018**, *301*, 1618–1627. [CrossRef]
17. Hopf, A.; Schaefer, D.J.; Kalbermatten, D.F.; Guzman, R.; Madduri, S. Schwann Cell-Like Cells: Origin and Usability for Repair and Regeneration of the Peripheral and Central Nervous System. *Cells* **2020**, *9*, 1990. [CrossRef] [PubMed]
18. Yuan, Q.; Liao, D.; Yang, X.; Li, X.; Wei, N.; Tan, Z.; Gong, P. Effect of Implant Surface Microtopography on Proliferation, Neurotrophin Secretion, and Gene Expression of Schwann Cells. *J. Biomed. Mater. Res. A* **2010**, *93*, 381–388. [CrossRef] [PubMed]
19. A, L.; Xu, W.; Zhao, J.; Li, C.; Qi, M.; Li, X.; Wang, L.; Zhou, Y. Surface Functionalization of TiO_2 Nanotubes with Minocycline and Its in Vitro Biological Effects on Schwann Cells. *Biomed. Eng. Online* **2018**, *17*, 88. [CrossRef]
20. Mishra, S.K.; Chowdhary, R.; Chrcanovic, B.R.; Brånemark, P.-I. Osseoperception in Dental Implants: A Systematic Review. *J. Prosthodont.* **2016**, *25*, 185–195. [CrossRef]
21. Habre-Hallage, P.; Dricot, L.; Jacobs, R.; van Steenberghe, D.; Reychler, H.; Grandin, C.B. Brain Plasticity and Cortical Correlates of Osseoperception Revealed by Punctate Mechanical Stimulation of Osseointegrated Oral Implants during FMRI. *Eur. J. Oral Implantol.* **2012**, *5*, 175–190.
22. Yan, C.; Ye, L.; Zhen, J.; Ke, L.; Gang, L. Neuroplasticity of Edentulous Patients with Implant-Supported Full Dentures. *Eur. J. Oral Sci.* **2012**, *116*, 387–393. [CrossRef] [PubMed]
23. Sun, S.; Diggins, N.H.; Gunderson, Z.J.; Fehrenbacher, J.C.; White, F.A.; Kacena, M.A. No Pain, No Gain? The Effects of Pain-Promoting Neuropeptides and Neurotrophins on Fracture Healing. *Bone* **2020**, *131*, 115109. [CrossRef] [PubMed]
24. Gittens, R.A.; McLachlan, T.; Olivares-Navarrete, R.; Cai, Y.; Berner, S.; Tannenbaum, R.; Schwartz, Z.; Sandhage, K.H.; Boyan, B.D. The effects of combined micron-/submicron-scale surface roughness and nanoscale features on cell proliferation and differentiation. *Biomaterials* **2011**, *32*, 3395–3403. [CrossRef]
25. Li, X.; Wang, M.; Zhang, W.; Bai, Y.; Liu, Y.; Meng, J.; Zhang, L. A Magnesium-Incorporated Nanoporous Titanium Coating for Rapid Osseointegration. *Int. J. Nanomed.* **2020**, *15*, 6593–6603. [CrossRef] [PubMed]
26. Buser, D.; Broggini, N.; Wieland, M.; Schenk, R.; Denzer, A.; Cochran, D.; Hoffmann, B.; Lussi, A.; Steinemann, S. Enhanced bone apposition to a chemically modified SLA titanium surface. *J. Dent. Res.* **2004**, *83*, 529–533. [CrossRef] [PubMed]
27. Liu, C.; Li, X.; Zhao, Q.; Xie, Y.; Yao, X.; Wang, M.; Cao, F. Nanofibrous Bicomponent Scaffolds for the Dual Delivery of NGF and GDNF: Controlled Release of Growth Factors and Their Biological Effects. *J. Mater. Sci. Mater. Med.* **2021**, *32*, 9. [CrossRef] [PubMed]
28. Wu, Z.; Pu, P.; Su, Z.; Zhang, X.; Nie, L.; Chang, Y. Schwann Cell-derived exosomes promote bone regeneration and repair by enhancing the biological activity of porous Ti6Al4V scaffolds. *Biochem. Biophys. Res. Commun.* **2020**, *531*, 559–565. [CrossRef] [PubMed]